Immunity, Volume *44*

Supplemental Information

The Proteomic Landscape of Human Ex Vivo Regulatory and Conventional T Cells Reveals Specific Metabolic Requirements

Claudio Procaccini, Fortunata Carbone, Dario Di Silvestre, Francesca Brambilla, Veronica De Rosa, Mario Galgani, Deriggio Faicchia, Gianni Marone, Donatella Tramontano, Marco Corona, Carlo Alviggi, Antonio Porcellini, Antonio La Cava, Pierluigi Mauri, and Giuseppe Matarese

Supplemental Information

The Proteomic Landscape of Human Ex Vivo Regulatory and Conventional T Cells Reveals Specific Metabolic Requirements

Claudio Procaccini, Fortunata Carbone, Dario Di Silvestre, Francesca Brambilla, Veronica De Rosa, Mario Galgani, Deriggio Faicchia, Gianni Marone, Donatella Tramontano, Marco Corona, Carlo Alviggi, Antonio Porcellini, Antonio La Cava, Pierluigi Mauri, Giuseppe Matarese

INVENTORY OF SUPPLEMENTAL ITEMS

1) **Supplemental data**

Supplemental Figures

Figure S1: Map of the interactome networks of freshly-isolated Treg *vs* Tconv cells in the membranes/cytosol and analysis of proteins involved in glycolysis, lipid synthesis/transport, FAO and TCA cycle (related to **Figure 1**).

Figure S2: Map of the interactome networks of unstimulated Treg cells *vs* anti-CD3 and anti-CD28-stimulated Treg cells in the membranes and in the cytosol (related to **Figure 2**).

Figure S3: Map of the interactome networks of anti-CD3 and anti-CD28-stimulated Treg cells *vs* leptin-neutralized Treg cells in the membranes and in the cytosol (related to **Figure 2**).

Figure S4: Effects of 2-DG or etomoxir on Treg cell proliferation and survival, and analysis of the metabolic asset of *in vitro* cultured Treg cells in the presence or absence of leptin neutralization (related to **Figure 3**).

Figure S5: Map of the interactome networks of unstimulated Tconv cells *vs* anti-CD3 and anti-CD28-stimulated Tconv cells in the membranes and in the cytosol (related to **Figure 5**).

Figure S6: Map of the interactome networks of anti-CD3 and anti-CD28-stimulated Tconv cells *vs* leptin-neutralized Tconv cells in the membranes and in the cytosol (related to **Figure 5**).

Figure S7: Effects of 2-DG or etomoxir on Tconv cell proliferation and survival and analysis of the metabolic asset of *in vitro* cultured Tconv cells in the presence or absence of leptin neutralization (related to **Figures 6** and **7**).

Supplemental Tables

Table S1. Data set of all the differentially represented proteins in freshly-isolated Treg *vs* Tconv cells in the membranes (**A**), in the cytosol (**B**) and list of selected differentially represented proteins (**C**) (related to **Figure 1** and **Figure S1**).

Table S2. Data set of all the differentially represented proteins in anti-CD3 and anti-CD28-stimulated *vs* unstimulated Treg cells in the membranes (**A**), in the cytosol (**B**) and list of selected differentially represented proteins (**C**) (related to **Figure 2**).

Table S3. Data set of all the differentially represented proteins in anti-CD3 and anti-CD28-stimulated *vs* leptin-neutralized Treg cells in the membranes (**A**), in the cytosol (**B**) and list of selected differentially represented proteins (**C**) (related to **Figure 2**).

Table S4. Data set of all the differentially represented proteins in anti-CD3 and anti-CD28-stimulated *vs* unstimulated Tconv cells in the membranes (**A**), in the cytosol (**B**) and list of selected differentially represented proteins (**C**) (related to **Figure 5**).

Table S5. Data set of all the differentially represented proteins in anti-CD3 and anti-CD28-stimulated *vs* leptin-neutralized Tconv cells in the membranes (**A**), in the cytosol (**B**) and list of selected differentially represented proteins (**C**) (related to **Figure 5**).

2) Supplemental Experimental Procedures

- Tryptic digestion
- Mass spectrometry
- Data handling for proteomic analyses
- Network analysis
- Mitochondrial bioenergetics and metabolic assays
- "In-Seahorse" leptin neutralization
- Annexin V/PI staining
- Intracellular cytokines staining
- Statistical analysis

3) Supplemental References

Freshly-isolated Treg *vs* Tconv

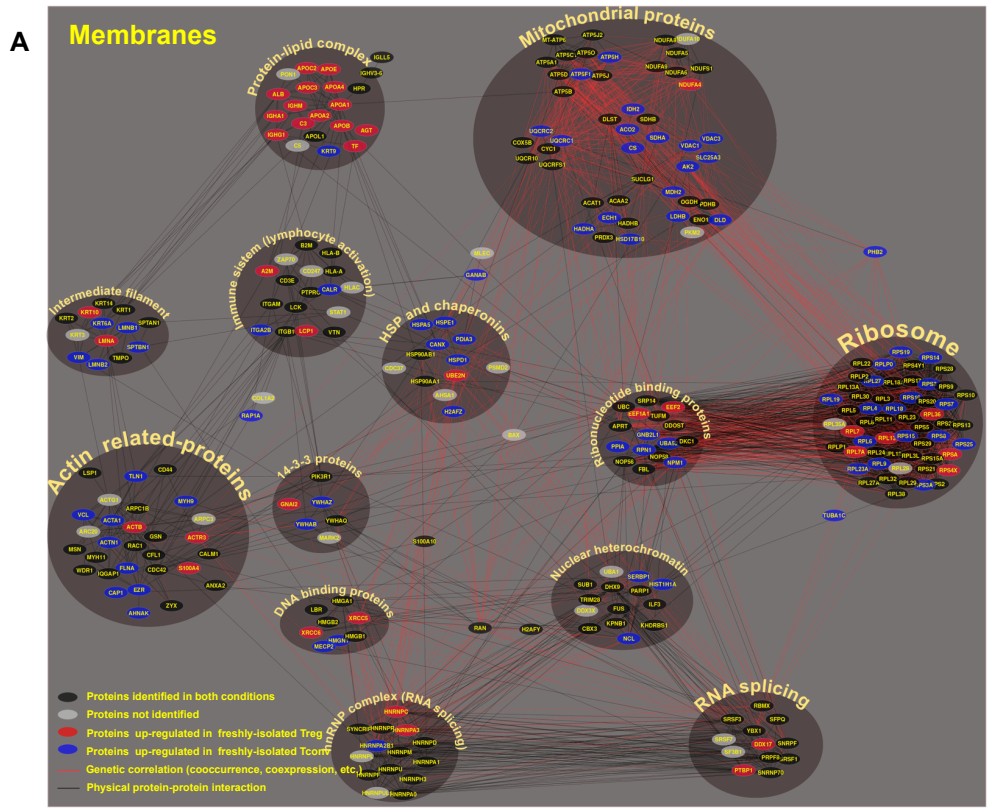

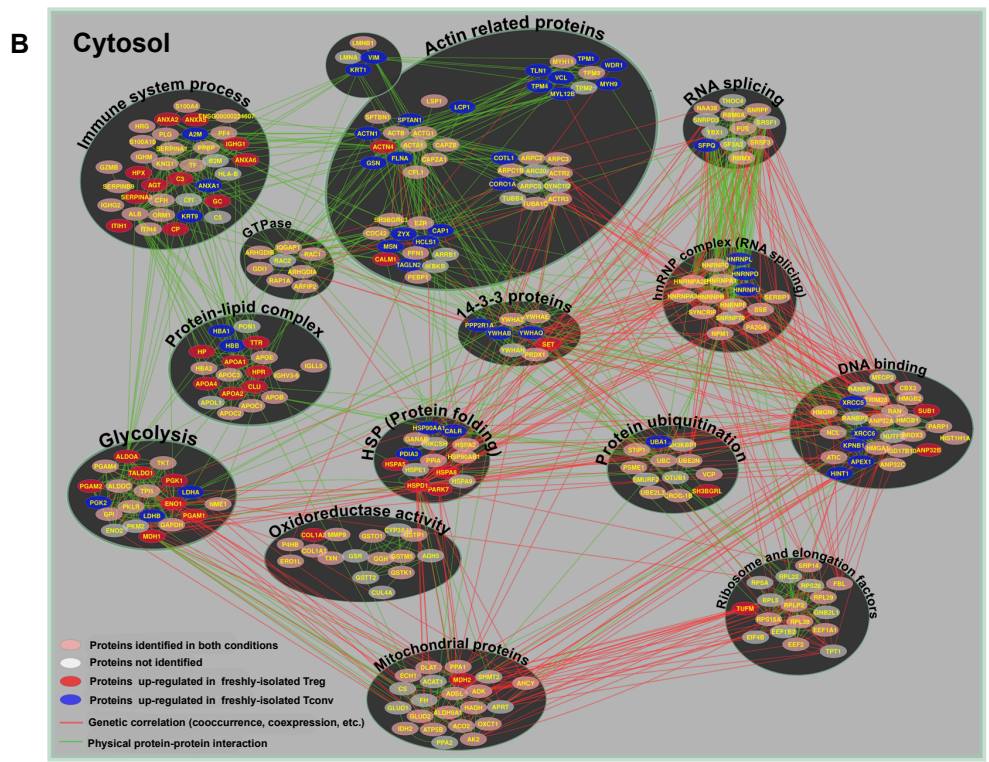

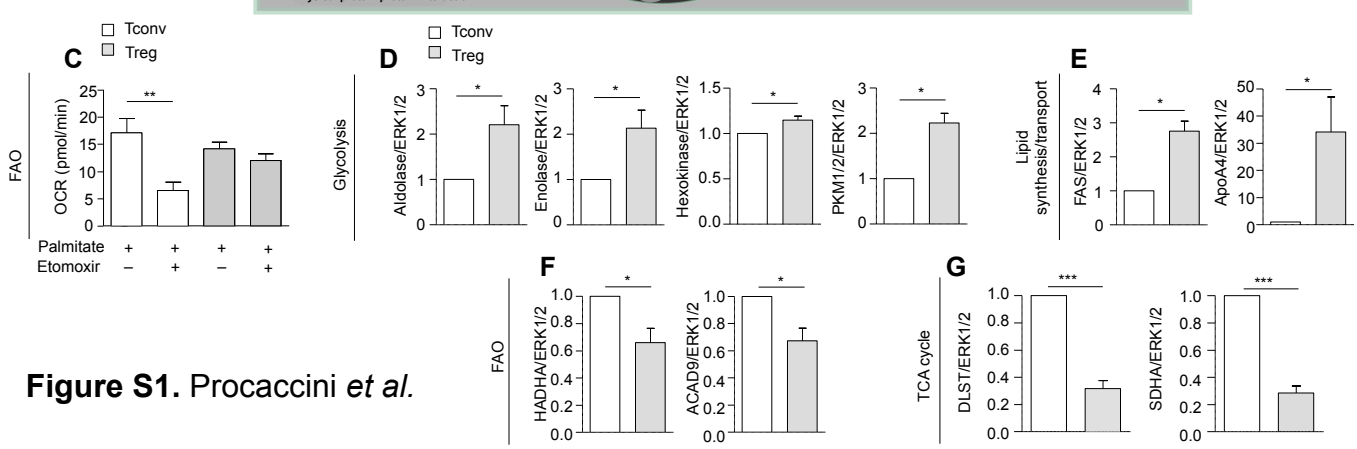

Figure S1. Procaccini *et al.*

Treg anti-CD3/CD28 *vs* Medium

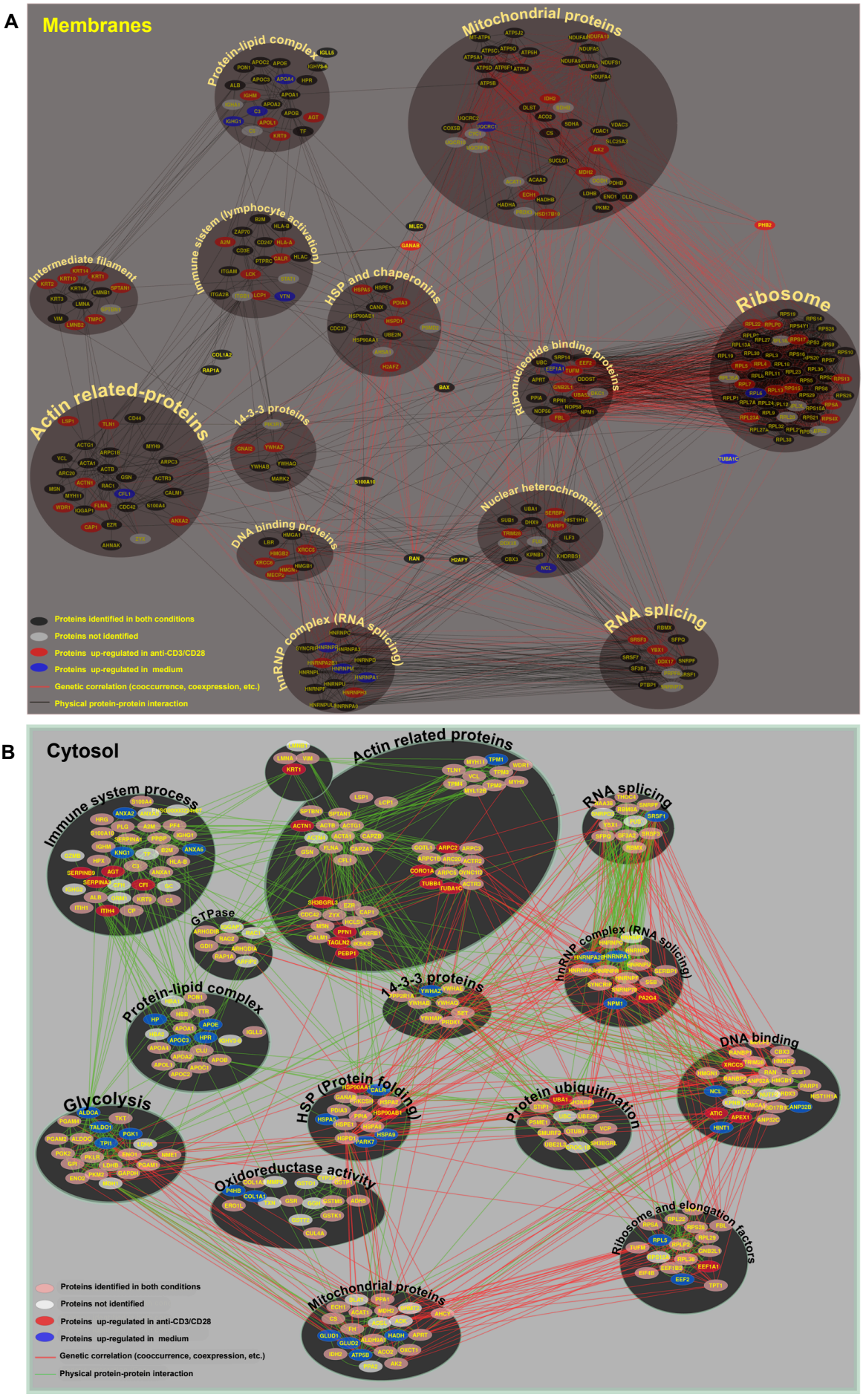

Figure S2. Procaccini *et al.*

Treg anti-CD3/CD28 *vs* Anti-leptin

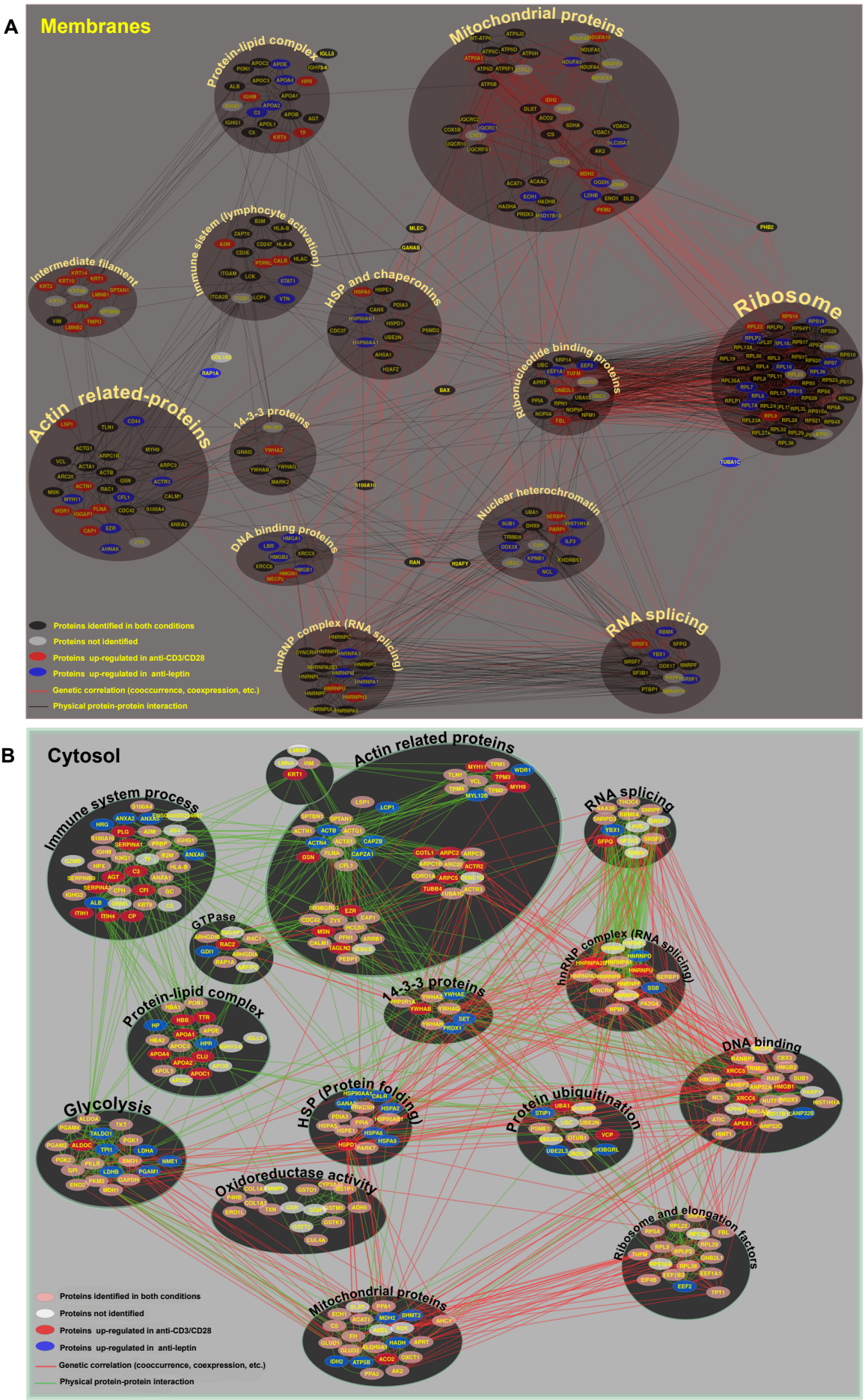

Figure S3. Procaccini *et al.*

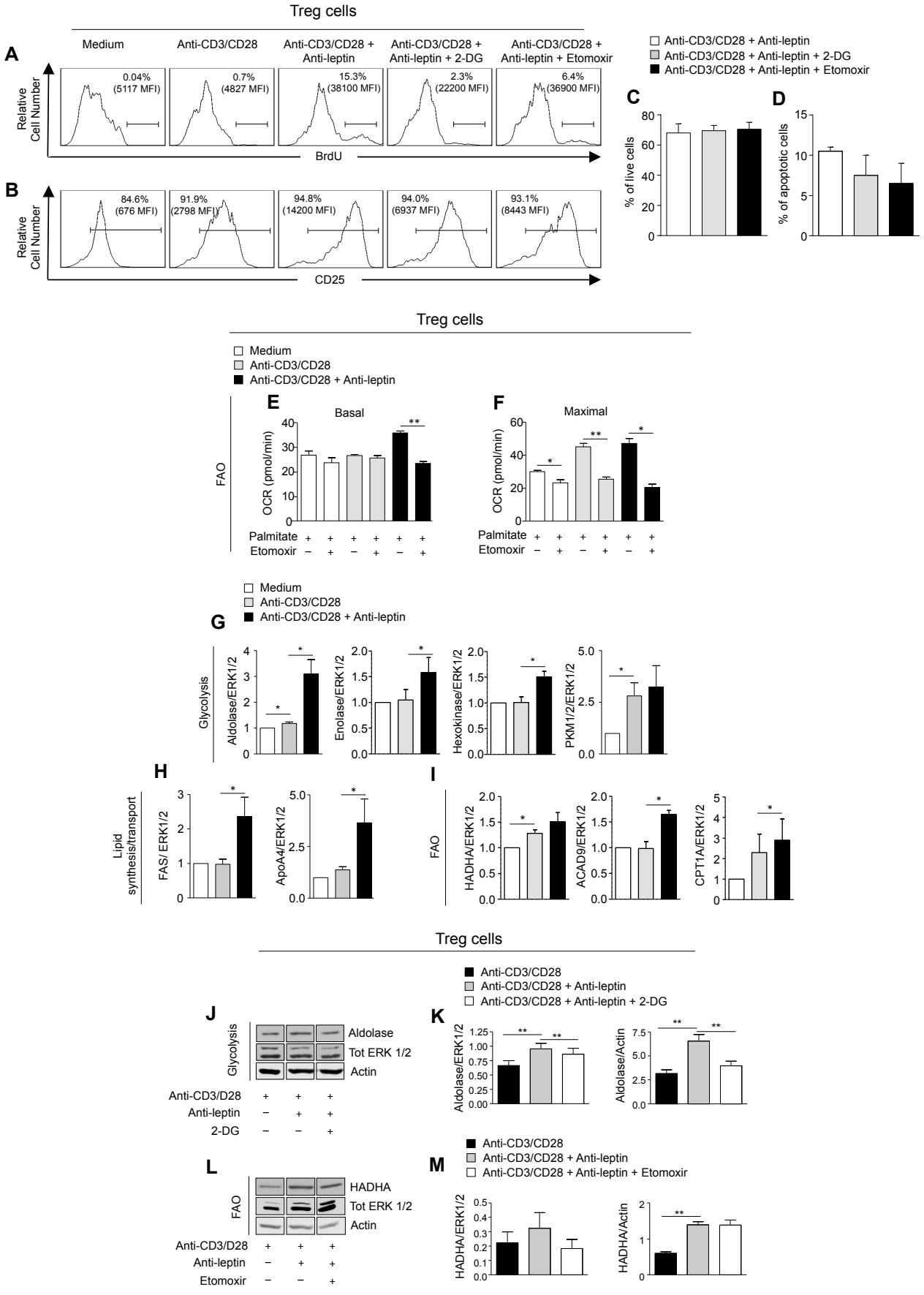

Figure S4. Procaccini *et al.*

Tconv anti-CD3/CD28 *vs* Medium

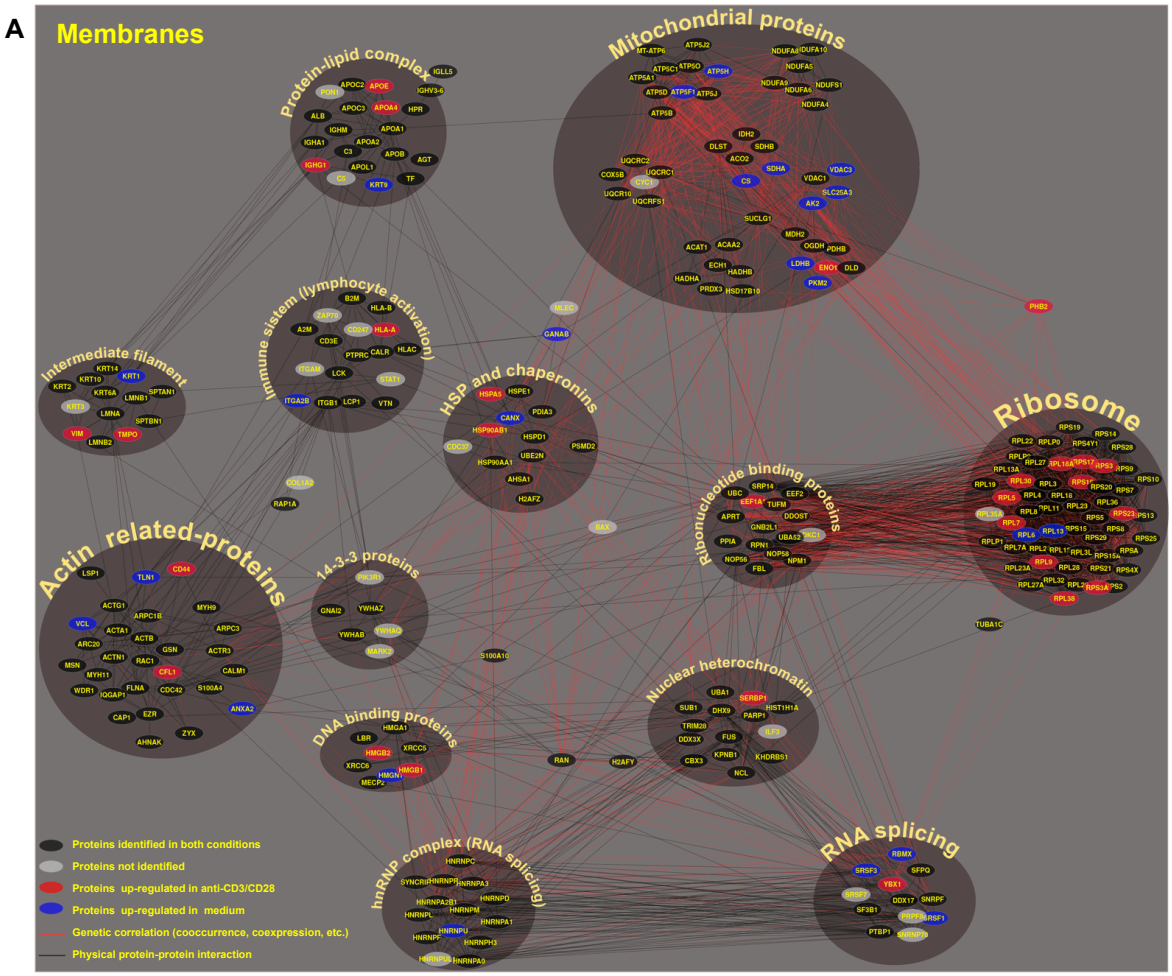

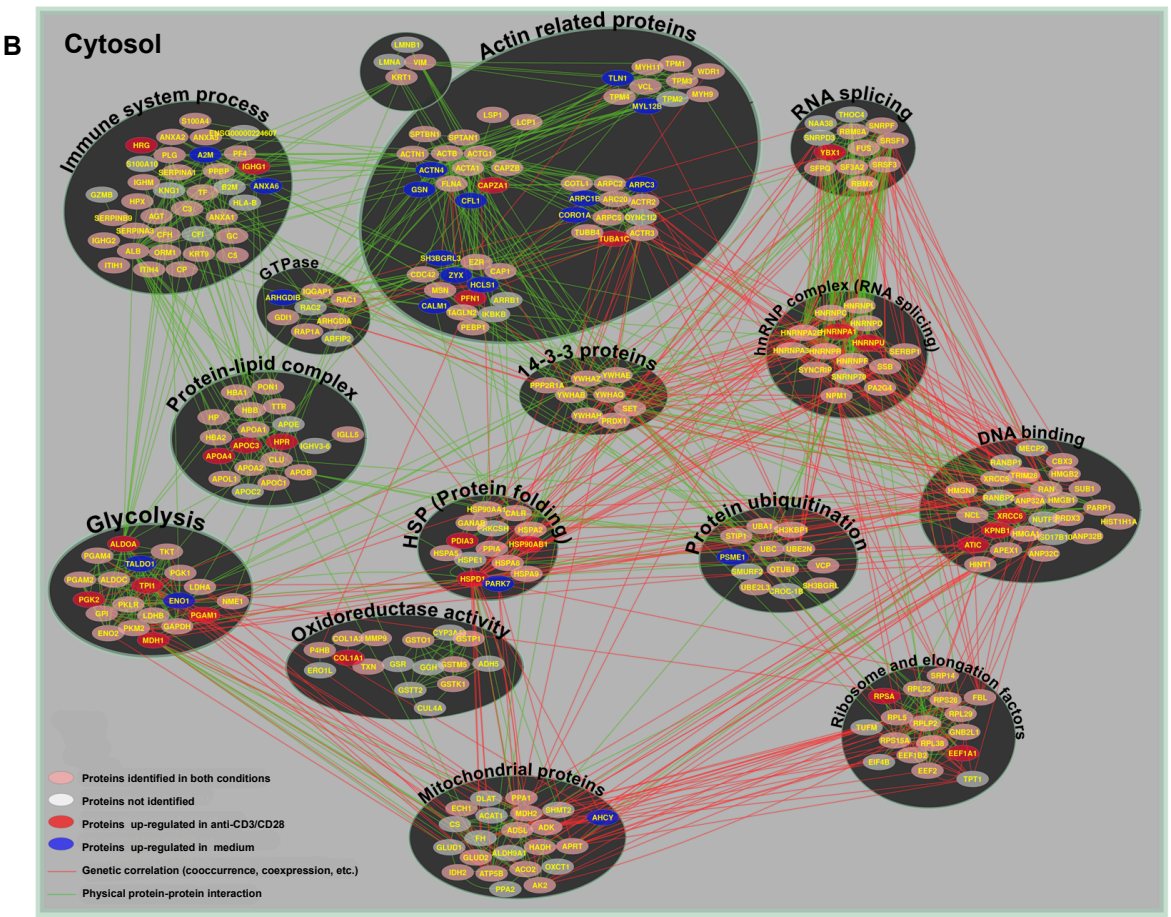

Figure S5. Procaccini *et al.*

Tconv anti-CD3/CD28 *vs* Anti-leptin

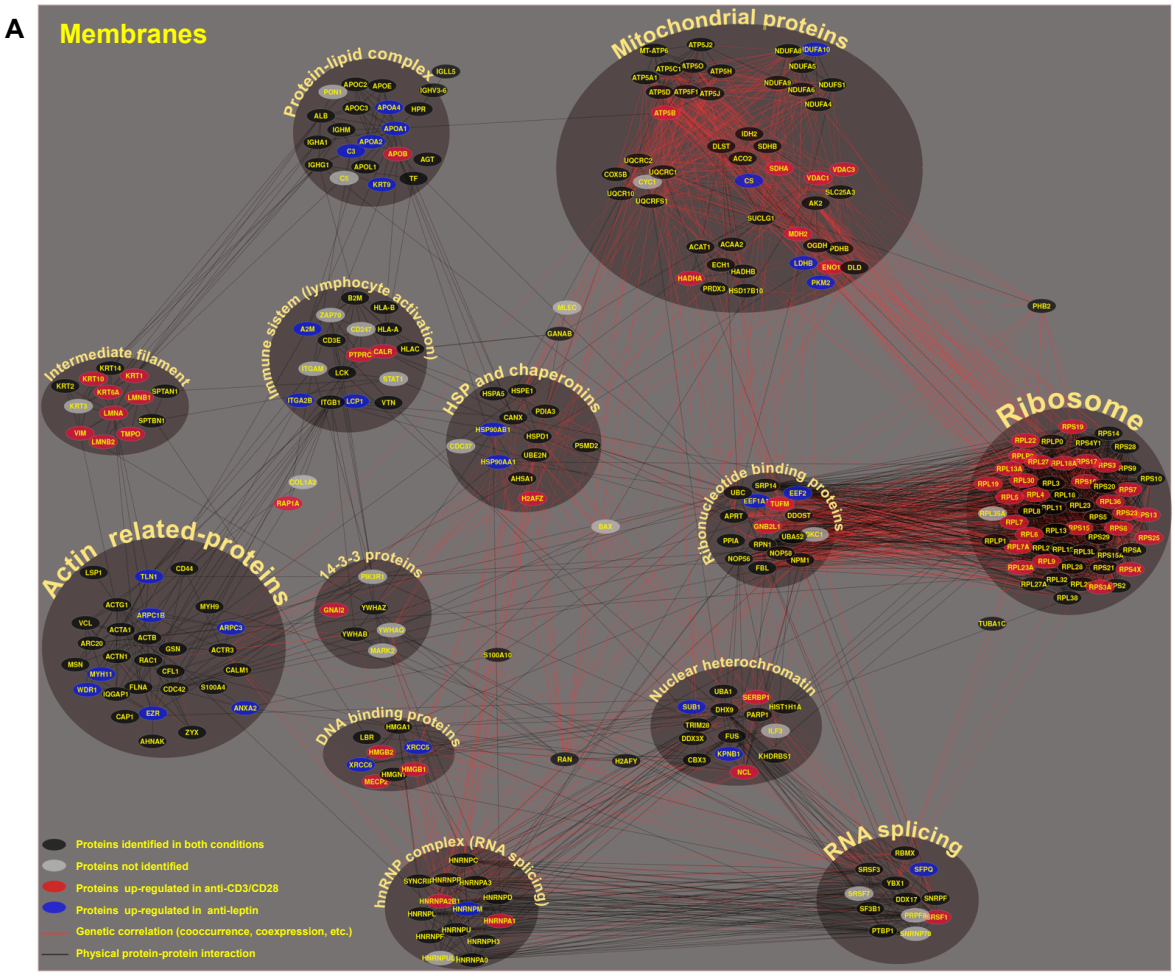

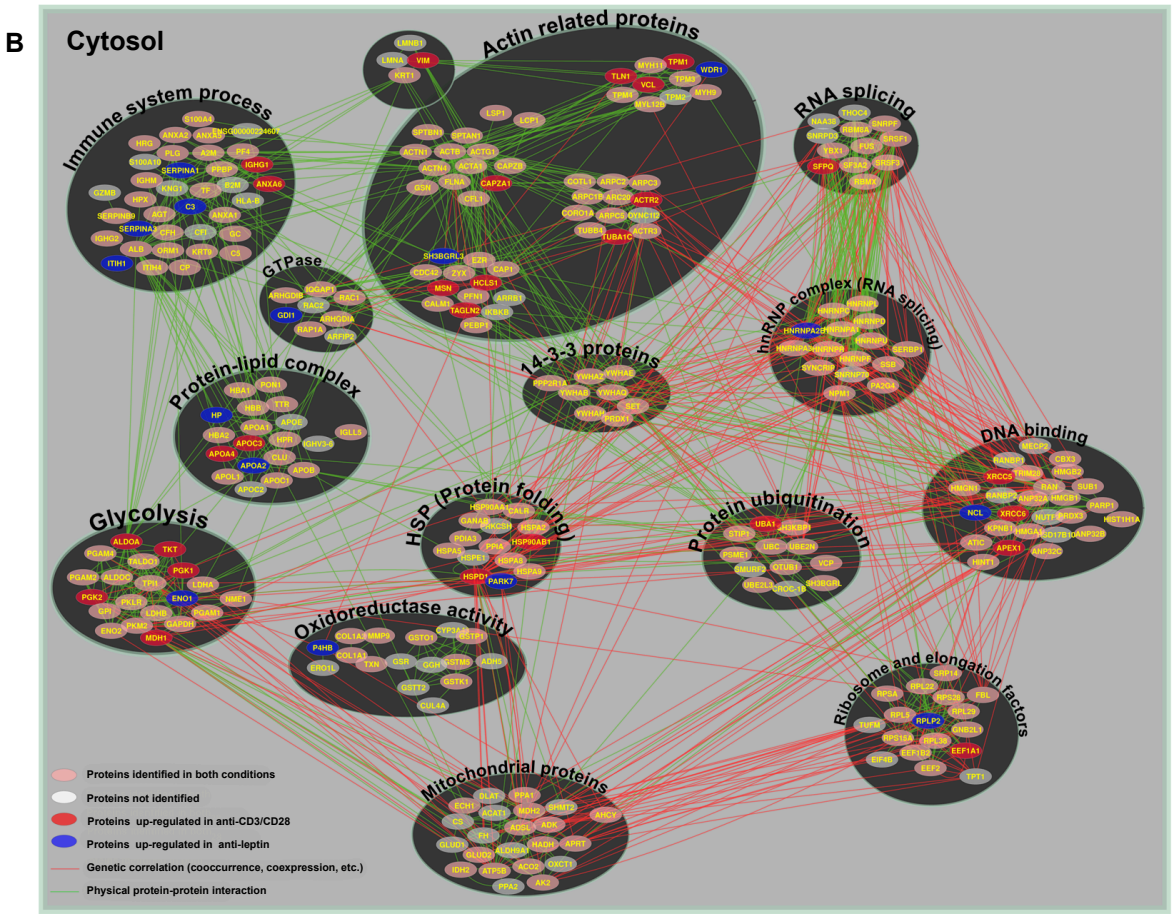

Figure S6. Procaccini *et al.*

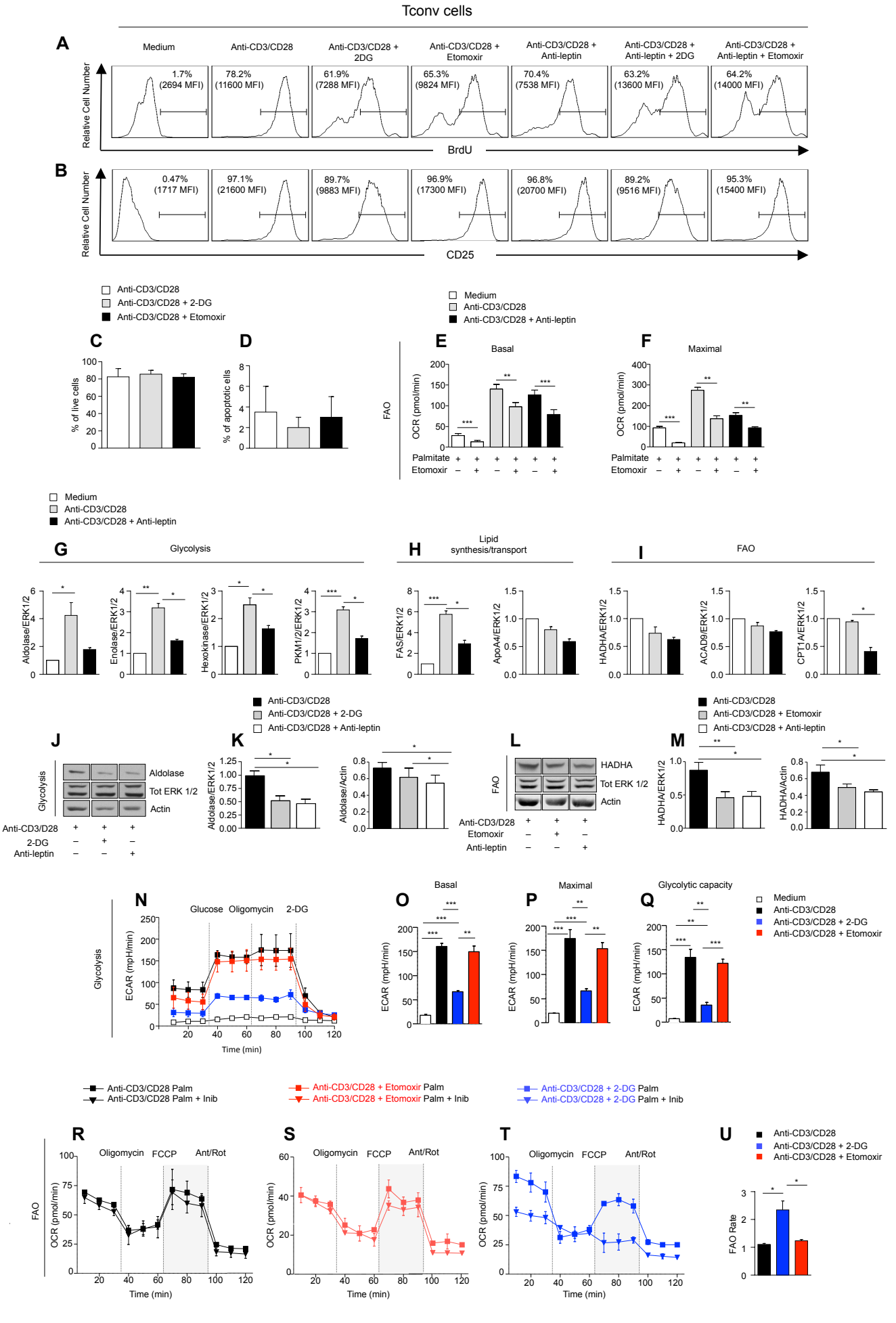

Figure S7. Procaccini *et al.*

Supplementary Figure legend

Figure S1. Map of the interactome networks of freshly-isolated Treg *vs* Tconv cells in the membranes/cytosol and analysis of proteins involved in glycolysis, lipid synthesis/transport, FAO and TCA cycle. Map of the interactome networks divided in several functional classes, obtained by comparing the protein profile of freshly-isolated Tconv and Treg cells in the membranes (**A**) and in the cytosol (**B**). Red plots correspond to specific proteins upregulated in Treg cells; blue plots correspond to proteins upregulated in Tconv cells; black (**A**) or pink (**B**) plots represent the equally distributed proteins in the two cell compartments; gray plots are the not-identified proteins. Red lines represent genetic interactions, gray (**A**) or green (**B**) lines represent protein-protein interaction. **C)** FAO in freshly-isolated Tconv (white columns) and Treg (gray columns) cells. This parameter was calculated as the difference between OCR in the presence of palmitate and OCR in the presence of palmitate + etomoxir (one representative out of three independent experiments). Data are expressed as mean ± S.E.M. of three measurements, each of them in triplicates. Statistical analysis by paired two-tailed Student's *t*-test (**$p < 0.005$). **D-G)** The graphs show the relative densitometric quantitation of aldolase, enolase, hexokinase, PKM1/2, FAS, ApoA4, HADHA, ACAD9, DLST and SDHA normalized on total ERK 1/2 in freshly-isolated Tconv and Treg cells and shown as fold over Tconv cells (n = 6; data are shown as mean ± S.E.M. of two independent experiments, in triplicates). Statistical analysis by paired two-tailed Student's *t*-test (*$p < 0.05$, ***$p < 0.0001$).

Figure S2. Map of the interactome networks of unstimulated Treg cells *vs* anti-CD3 and anti-CD28-stimulated Treg cells in the membranes and in the cytosol. Map of the interactome networks divided in several functional classes, obtained by comparing the protein profile of unstimulated Treg cells with that of *in vitro* cultured Treg cells stimulated with anti-CD3 and anti-CD28 upon 12 hours culture, in the membranes (**A**) and the cytosol (**B**). Red plots correspond to specific proteins upregulated in anti-CD3 and anti-CD28 stimulated Treg cells; blue plots

correspond to proteins upregulated in unstimulated Treg cells; black (**A**) or pink (**B**) plots represent the equally distributed proteins in the two conditions; gray plots are the not-identified proteins. Red lines represent genetic interactions, gray (**A**) or green (**B**) lines represent protein-protein interaction.

Figure S3. Map of the interactome networks of anti-CD3 and anti-CD28-stimulated Treg cells *vs* leptin-neutralized Treg cells in the membranes and in the cytosol. Map of the interactome networks divided in several functional classes, obtained by comparing the protein profile of anti-CD3 and anti-CD28-stimulated Treg cells with that of leptin-neutralized Treg cells upon 12 hours culture, in the membranes (**A**) and the cytosol (**B**). Red plots correspond to specific proteins upregulated in anti-CD3 and anti-CD28 stimulated Treg cells; blue plots correspond to proteins upregulated in leptin-neutralized Treg cells; black (**A**) or pink (**B**) plots represent the equally distributed proteins in the two conditions; gray plots are the not-identified proteins. Red lines represent genetic interactions, gray (**A**) or green (**B**) lines represent protein-protein interaction.

Figure S4. Effects of 2-DG or etomoxir on Treg cell proliferation and survival, and analysis of the metabolic asset of *in vitro* cultured Treg cells in the presence or absence of leptin neutralization. Representative flow cytometry plots showing BrdU (**A**) and CD25 (**B**) expression in Treg cells upon 72h anti-CD3 and anti-CD28 stimulation in the presence or absence of leptin-neutralizing antibody, 2-DG or etomoxir. Percentage and MFI of positive cells are indicated. One representative out of three independent experiments. Percentage of live Treg cells (**C**) and apoptotic Treg cells (**D**) (evaluated by Annexin V/PI staining) upon 72h anti-CD3 and anti-CD28 stimulation with leptin-neutralizing antibody, in the presence or absence of 2-DG or etomoxir. The data are shown as mean ± S.E.M. of two independent experiments. Statistical analysis by two tailed-Student *t* test. **(E-F)** FAO in unstimulated (white columns), anti-CD3 and anti-CD28-stimulated (gray columns) and leptin-neutralized Treg cells (black columms). This parameter was calculated as the difference between OCR in the presence of palmitate and OCR in the presence of palmitate +

etomoxir, in basal conditions (**E**) and during maximal respiration conditions (**F**), upon FCCP-stimulation (one representative out of three independent experiments) (n = 6; data are shown as mean ± S.E.M. of three measurements, each of them in duplicates. Statistical analysis by paired two-tailed Student's *t*-test (*$p < 0.05$, **$p < 0.001$). **G-I**) The graphs show the relative densitometric quantitation of aldolase, enolase, hexokinase, PKM1/2, FAS, ApoA4, HADHA, ACAD9, CPT1A normalized on total ERK 1/2 in unstimulated (white columns), anti-CD3 and anti-CD28-stimulated (gray columns) and leptin-neutralized Treg cells (black columms) and shown as fold over unstimulated Treg cells (n = 6; data are shown as mean ± S.E.M. of two independent experiments, in triplicates). Statistical analysis by paired two-tailed Student's *t*-test (*$p < 0.05$). **(J)** Immunoblot for aldolase, and (**K**) its relative densitometric quantitation (on actin and total ERK 1/2), on Treg cells upon 12h anti-CD3 and anti-CD28 stimulation in the presence or absence of leptin-neutralizing antibody and 2-DG. Actin and total ERK 1/2 served as a loading control. (**L**) Immunoblot for HADHA, and (**M**) its relative densitometric quantitation (on actin and total ERK 1/2) on Treg cells upon 12h anti-CD3 and anti-CD28 stimulation in the presence or absence of leptin-neutralizing antibody and etomoxir. Actin and total ERK 1/2 served as a loading control (n = 4). In **K** and **M** panels the data are shown as mean ± S.E.M. of two independent experiments, in duplicates. Statistical analysis by paired two-tailed Student's *t*-test (**$p < 0.005$).

Figure S5. Map of the interactome networks of unstimulated Tconv cells *vs* anti-CD3 and anti-CD28-stimulated Tconv cells in the membranes and in the cytosol. Map of the interactome networks divided in several functional classes, obtained by comparing the protein profile of unstimulated Tconv cells with that of *in vitro* cultured Tconv cells stimulated with anti-CD3 and anti-CD28 upon 12 hours culture in the membranes (**A**) and in the cytosol (**B**). Red plots correspond to specific proteins upregulated in anti-CD3 and anti-CD28 stimulated Tconv cells; blue plots correspond to proteins upregulated in unstimulated Tconv cells; black (**A**) or pink (**B**) plots represent the equally distributed proteins in the two conditions; gray plots are the not-identified

proteins. Red lines represent genetic interactions, gray (**A**) or green (**B**) lines represent protein-protein interaction.

Figure S6. **Map of the interactome networks of anti-CD3 and anti-CD28-stimulated Tconv cells *vs* leptin-neutralized Tconv cells in the membranes and in the cytosol.** Map of the interactome networks divided in several functional classes, obtained by comparing the protein profile of anti-CD3 and anti-CD28-stimulated Tconv cells and that of leptin-neutralized Tconv cells upon 12 hours culture in the membranes (**A**) and in the cytosol (**B**). Red plots correspond to specific proteins upregulated in anti-CD3 and anti-CD28 stimulated Tconv cells; blue plots correspond to proteins upregulated in leptin-neutralized Tconv cells; black (**A**) or pink (**B**) plots represent the equally distributed proteins in the two conditions; gray plots are the not-identified proteins. Red lines represent genetic interactions, gray (**A**) or green (**B**) lines represent protein-protein interaction.

Figure S7. Effects of 2-DG or etomoxir on Tconv cell proliferation and survival and analysis of the metabolic asset of *in vitro* cultured Tconv cells in the presence or absence of leptin neutralization. Representative flow cytometry plots showing BrdU (**A**) and CD25 (**B**) expression in Tconv cells upon 72h anti-CD3 and anti-CD28 stimulation in the presence or absence of leptin-neutralizing antibody, 2-DG or Etomoxir. Percentage and MFI of positive cells are indicated. One representative out of three independent experiments. Percentage of live Tconv cells (**C**) and apoptotic Tconv cells (**D**) (evaluated by Annexin V/PI staining) upon 72h anti-CD3 and anti-CD28 stimulation in the presence or absence of 2-DG or Etomoxir. The data are shown as mean ± S.E.M. of two independent experiments. Statistical analysis by two tailed-Student *t* test. (**E-F)** FAO in unstimulated (white columns), anti-CD3 and anti-CD28-stimulated (gray columns) and leptin-neutralized Tconv cells (black columms). This parameter was calculated as the difference between OCR in the presence of palmitate and OCR in the presence of palmitate + etomoxir, in basal conditions (**E**) and during maximal respiration conditions (**F**), upon FCCP-stimulation (one

representative out of three independent experiments). (n = 6; data are shown as mean ± S.E.M. of three measurements, each of them in duplicates). Statistical analysis by two tailed paired *t* test (***p* < 0.001, ****p* < 0.0001). **G-I**) The graphs show the relative densitometric quantitation of Aldolase, Enolase, Hexokinase, PKM1/2, FAS, ApoA4, HADHA, ACAD9, CPT1A normalized on total ERK 1/2 in unstimulated (white columns), anti-CD3 and anti-CD28-stimulated (gray columns) and leptin-neutralized Tconv cells (black columms) and shown as fold over unstimulated Tconv cells. (n = 6; data are shown as mean ± S.E.M. of two independent experiments, in triplicates). Statistical analysis by paired two-tailed Student's *t*-test (**p* < 0.05, ***p* < 0.001, ****p* < 0.0001). **(J)** Immunoblot for aldolase, and (**K**) its relative densitometric quantitation (on actin and total ERK 1/2), on Tconv cells upon 12h anti-CD3 and anti-CD28 stimulation in the presence or absence of leptin-neutralizing antibody and 2-DG. Actin and total ERK 1/2 served as a loading control. (**L**) Immunoblot for HADHA and (**M**) its relative densitometric quantitation (on actin and ERK 1/2) on Tconv cells upon 12h anti-CD3 and anti-CD28 stimulation in the presence or absence of leptin-neutralizing antibody and etomoxir. Actin and total ERK 1/2 served as a loading control. (n = 4, data are shown as mean ± S.E.M. of two independent experiments, in duplicates). (**K** and **M**) Statistical analysis by paired two-tailed Student's *t*-test (**p* < 0.05, ***p* < 0.001). (**N**) Kinetic profile of ECAR in Tconv cells stimulated or not with anti-CD3 and anti-CD28 for 12h, in the presence or absence of 2-DG or etomoxir (one representative out of three independent experiments). The data are shown as mean ± S.E.M. of triplicates. ECAR was measured in real time, under basal conditions and in response to glucose, oligomycin and 2-DG. Indices of glycolytic pathway activation, calculated from Tconv cells ECAR profile: basal ECAR (**O**), maximal ECAR (**P**) and glycolytic capacity (**Q**) in Tconv cells stimulated for 12h with anti-CD3 and anti-CD28, in the presence or absence of 2-DG or etomoxir. (n = 9, data are shown as mean ± S.E.M. of three measurements, each of them in triplicates). Statistical analysis by paired two-tailed Student's *t*-test (***p* < 0.001, ****p* < 0.0001). OCR quantifying FAO of 12h anti-CD3 and anti-CD28-stimulated Tconv cells (**R**), 12h cultured in the presence of anti-CD3 and anti-CD28 + etomoxir (**S**) or 2-DG (**T**). One representative

out of three independent experiments. Graphs are shown as mean ± S.E.M. of duplicates. (**U**) FAO index, calculated as ratio between FCCP-stimulated OCR in the presence of palmitate and FCCP-stimulated OCR in the presence of palmitate plus inhibitor (etomoxir). The gray panels highlight the values used to calculate FAO rate. (n = 6; data are shown as mean ± S.E.M. of three measurements, each of them in duplicates) *$p < 0.05$ by paired two-tailed Student's *t*-test. Palm: palmitate; Inhib: etomoxir.

Supplemental Experimental Procedures

Tryptic digestion

Supernatant and pellet samples were treated with RapiGest^{TM} SF (Waters Corporation, Milford, MA, USA) at the final concentration of 0.2% (w/v) in 0.1M NH_4HCO_3. After incubation at 100°C for 5 min, they were cooled to room temperature, protein concentration was determined (SPN^{TM} – Protein Assay, G-Biosciences, St. Louis, MO, USA) and each sample was digested with trypsin (Sequencing Grade Modified Trypsin, Promega, Madison, WI, USA). Initially, it was added to mixtures at an enzyme/substrate ratio of about 1:50 (w/w) and incubated at 37°C overnight. Then, another aliquot of trypsin was added at an enzyme/substrate ratio of 1:100 (w/w) and samples were further incubated at 37°C for 4 hours. Trypsin digestion was stopped by the addition of 0.5% TFA (Sigma-Aldrich Inc., St. Louis, MO, USA, and subsequent incubation at 37°C for 45 min. Centrifugation at 13,000 x g for 10 min removed hydrolytic RapiGest^{TM} SF by-products. Finally, before MudPIT analysis, samples were desalted by PepClean C-18 spin columns (Pierce Biothecnology Inc., Rockford, IL, USA), concentrated in a SpeedVac (Savant Instruments Farmingdale, NY, USA) at 60°C and resuspended in 0.1% formic acid (Sigma-Aldrich Inc., St. Louis, MO, USA).

Mass spectrometry

Trypsin-digested samples were analyzed by two dimensional liquid chromatography coupled to tandem mass spectrometry (Multidimensional Protein Identification Technology, MudPIT) (Mauri and Scigelova, 2009). Two technical replicates were performed for each biological sample. Briefly, 3 µg of peptide mixture were loaded, by means of an autosampler (Suveyor AS Thermo), onto a strong cation exchange column (BioBasic-SCX, 0.32 i.d. x 100 mm, 5µm, Thermo Electron Corporation, Bellofonte, PA, USA) and then eluted using eight steps of increasing ammonium chloride concentration (0, 20, 40, 80, 120, 200, 400, 700 mM). Peptides eluted by each salt steps were first captured in turn onto two peptide traps (Zorbax 300 SB C-18, 5 µm, 0.3 id x 5 mm, Agilent technologies, Santa Clara, CA, USA) mounted on a 10-port valve, for concentration and desalting, and subsequently loaded on a reversed phase C-18 column (BioBasic-18, 0.180 i.d. x 100 mm, 5 µm, Thermo Electron Corporation, Bellofonte, PA, USA) for separation by means of an acetonitrile gradient (eluent A, 0.1% formic acid in water; eluent B, 0.1% formic acid in acetonitrile; the gradient profile was started and kept for 3 min at 5% eluent B, followed by 5–65% eluent B within 43 minutes and finally ramped to 95% eluent B for 6 minutes). The flow rate was 100 µl/min split in order to achieve a final flux of 1 µl/min on C18 column. Peptides eluted from the C-18 column were directly analyzed by a mass spectrometer equipped with a NSI-ESI ion source and LTQ-Orbitrap^{XL} mass analyzer (ThermoFisher Scientific, San Josè, CA, USA). The heated capillary was held at 185°C; full mass spectra were acquired at high resolution (R=60000), in positive mode and over a 400-1600 *m/z* range, followed by four MS/MS events sequentially generated in data-dependent manner on the four most-intense ions selected from the full MS spectrum, using dynamic exclusion for MS/MS analysis (collision energy 35%).

Data handling for proteomic analyses

The experimental tandem mass spectra obtained by MudPIT analyses were correlated to tryptic peptide sequences by comparing them against theoretical mass spectra reconstructed by the

in silico digestion of *Homo sapiens* protein database. Data processing was performed using the 3.3.1 Bioworks version, based on SEQUEST (Washburn et al., 2001) algorithm (University of Washington, licensed to Thermo Finnigan Corp., San Josè, CA, USA), and the following parameters: Xcorr greater than 1.5 for single charged peptide ions, and 2.0 and 2.5 for doubly and triply charged ions, respectively; the peptide probability $\leq 1E^{-3}$ and the protein consensus score value ≥ 10. Using the same thresholds and a decoy database (Wang et al., 2009), consisting of *Homo sapiens* reverse protein sequences, false positive rate was estimated resulting less than 3%.

Protein lists obtained by SEQUEST were further processed with an in-house software called MAProMa (Mauri and Dehò, 2008) (Multidimensional Algorithm Protein Map). It permitted the alignment of protein lists of replicate analyses, the evaluation of the identification frequency and the semi-quantitative comparison of the analyzed conditions. In this context, differentially expressed proteins were selected by processing their SEQUEST Score by means of the DAVE (Differential Average) and DCI (Differential Coefficient Index) algorithms, available in MAProMa. Specifically, the threshold values imposed were DAve $\geq|0.2|$ and DCI$\geq|200|$ (Di Silvestre et al., 2013) DAve is an index of the ratio between the two compared protein list and DCI is an index to evaluate the confidence of DAve.

Network analysis

A global *Homo sapiens* protein interactomic network with more than 22,000 nodes and 200,000 interactions was built by means of the Cytoscape plugin Bionetbuilder (Avila-Campillo et al., 2007). This tool combined protein-protein interactions retrieved from major public online repositories, including HPRD, MINT, BioGrid, IntAct, DIP, BIND, KEGG, MPPI, and GO. All types of interactions were retrieved from each repository without applying a p-value threshold. However, if present, protein-DNA, protein-RNA, protein-metabolite and protein-drug interactions were removed, as well as duplicates and self-interactions. Starting from the list of experimentally identified proteins, the corresponding networks were extracted. Proteins not mapped or mapped as

isolated components weren't considered in the analysis. The networks were analysed using Cytoscape (Shannon et al., 2003) software. In particular, the Bingo 2.44 plugin (Maere et al., 2005) was used to emphasise sub-networks based on functionally organised GO terms, and the MCODE plugin (Bader and Hogue, 2003) was used to cluster sub-networks based on their topology and, specifically, by considering densely connected regions.

Mitochondrial bioenergetics and metabolic assays

The metabolic profile has been evaluated in freshly isolated Treg and Tconv, and in 12h cultured Treg and Tconv in the presence or absence of anti-CD3 and anti-CD28 stimulation, treated or not with leptin neutralizing antibody. Real-time measurements of oxygen consumption rate (OCR) and extracellular acidification rate (ECAR) were made using an XFe-96 Extracellular Flux Analyzer (Seahorse Bioscience). Cells were plated in XFe-96 plates (seahorse Bioscience) at the concentration of 2 x 10^5 cells/well and cultured for 12h in RPMI-1640 medium supplemented with 5% AB human serum. OCR was measured in XF media (non-buffered DMEM medium, containing 10 mM glucose, 2 mM L-glutamin, and 1 mM sodium pyruvate), under basal conditions and in response to 5 μM oligomycin, 1.5 μM of carbonylcyanide-4- (trifluoromethoxy) -phenylhydrazone (FCCP) and 1 μM of Antimycin and Rotenone (all from Sigma Aldrich). Indices of mitochondrial respiratory function were calculated from OCR profile: basal OCR (before addition of oligomycin), ATP-linked OCR (calculated as the difference between basal OCR rate and oligomycin-induced OCR rate) and maximal OCR (calculated as the difference of FCCP rate and antimycin+rotenone rate). ECAR was measured in XF media in basal condition and in response to 10 mM glucose, 5 μM oligomycin and 100 mM of 2-DG (all from Sigma Aldrich). Experiments with the Seahorse system were done with the following assay conditions: 3 min mixture; 3 minutes wait; and 3 min measurement. Metabolic parameters were then calculated. Data are expressed as mean and s.e.m. Indices of glycolytic pathway activationwere calculated from ECAR profile: basal ECAR (after the

addition of glucose), maximal ECAR (after the addition of oligomycin) and glycolytic capacity (calculated as the difference of oligomycin-induced ECAR and 2-DG-induced ECAR).

For the analysis of fatty acid oxidation (FAO) in all the above mentioned experimental condition, we used the XF Palmitate-BSA FAO substrate (Seahorse Bioscience). Briefly FAO was measured in FAO buffer containing NaCl 111 mM, KCl 4.7 mM, $MgSO_4$ 2.0 mM, Na_2HPO_4 1.2 mM, supplemented with 2.5 mM glucose, 0.5 mM carnitine and 5 mM HEPES (final concentrations) pH to 7.4. We added etomoxir (Sigma Aldrich) (40 μM final) 15 min pror to the XF assay being initiated (t = 0). At t = 0 cells were provided with 30 μl of 1mM Palmitate conjugated to 0.17 mM BSA. Determination of FAO was evaluated as the ratio between the value of FCCP-stimulated OCR in the presence of palmitate and the value of FCCP-stimulated OCR in the presence of etomoxir.

"In-Seahorse" leptin neutralization

To monitor the effect of leptin neutralization by metabolic flux analysis (i.e., in real time), anti-leptin mAb were directly applied into plated cells via the instrument's multi-injection ports. Antibody was injected 30 min after the experiment was initiated. The ECAR of Treg and Tconv was recorded for the duration of the experiment (100 min).

Annexin V/PI staining

For apoptosis staining experiments, Tconv and Treg cells were treated for 72h with 2-DG or etomoxir. 5×10^5 cells were harvested and stained according to the Tali Apoptosis Kit instructions (Invitrogen, Molecular Probes, Life Technologies). Briefly, cells were incubated with Annexin V Alexa Fluor 488 for 20 min at room temperature and then incubated for 5 min with Tali® Propidium Iodide. Fluorescence was scanned with the Tali Image based Cytometer (Invitrogen, Life Technologies). Apoptotic cells were Annexin V positive and the negative sample was acquired for control staining. The cells were analyzed using a Tali™ Image byuring captures 10 images of a

stained sample, automatically analyzes the images using digital image-based cell counting and fluorescence-detection algorithms, and displays an accurate quantitative analysis of live, dead, and apoptotic cell populations.

Intracellular cytokines staining

To analyze the production of IL-2 and IFN-γ, human Tconv cells were cultured overnight, with anti-CD3 and anti-CD28 in presence or absence of 2-DG (10 mM) or etomoxir (200 μM). To avoid extracellular cytokine export, the cultures were incubated overnight in the presence of 5 μg/ml of Brefeldin-A (Sigma–Aldrich). Intracellular staining with the mAbs recognising IL-2 (FITC, BD PharMingen, clone, MQ1-17H12 Cat.# 554563) and IFN-γ, (APC, BD PharMingen, clone, B27 Cat.# 554702) was performed by a BD Cytofix/Cytoperm (Cat. 554722) and BD Perm/Was (Cat. 554723), following the manufacturer's instructions.

Statistical analysis

The two tailed Mann-Whitney U-test was used for unrelated two-group analyses (comparison between Tconv and Treg cells) andt two tailed-paired *t* test for comparison of the different treatments in the same cellular subset, using StatView software (Abacus Concepts Inc.). Results are expressed as mean ± S.E.M. *P* values < 0.05 were considered statistically significant.

Supplemental references:

Avila-Campillo, I., Drew, K., Lin, J., Reiss D.J., and Bonneau R. (2007). BioNetBuilder: automatic integration of biological networks. Bioinformatics. *23*, 392-393.

Bader, G.D., and Hogue, C.W. (2003). An automated method for finding molecular complexes in large protein interaction networks. BMC Bioinformatics. *4*, 2.

Di Silvestre, D., Brambilla, F., and Mauri, P.L. (2013). Multidimensional protein identification technology for direct-tissue proteomics of heart. Methods Mol. Biol. *1005,* 25-38.

Maere, S., Heymans, K., and Kuiper, M. (2005). BiNGO: a Cytoscape plugin to assess overrepresentation of gene ontology categories in biological networks. Bioinformatics. *21*, 3448-3449.

Mauri, P., and Dehò, G. (2008). A proteomic approach to the analysis of RNA degradosome composition in Escherichia coli. Methods Enzymol. *447*, 99-117.

Mauri, P., and Scigelova, M. (2009). Multidimensional protein identification technology for clinical proteomic analysis. Clin. Chem. Lab. Med. *47*, 636-646.

Shannon, P., Markiel, A., Ozier, O., Baliga, N.S., Wang, J.T., Ramage, D., Amin, N., Schwikowski, B., Ideker, T. (2003). Cytoscape: a software environment for integrated models of biomolecular interaction networks. Genome Res. *13*, 2498-2504.

Wang, G., Wu, W.W., Zhang, Z., Masilamani, S., and Shen, R.F. (2009). Decoy methods for assessing false positives and false discovery rates in shotgun proteomics. Anal. Chem. *81*, 146-159.

Washburn, M.P., Wolters, D., and Yates, J.R. 3rd. (2001). Large-scale analysis of the yeast proteome by multidimensional protein identification technology. Nat. Biotechnol. *19*, 242-247.